

Comparison of Node Architectures for Elastic Optical Networks with Waveband Conversion

ZHANG Ping¹, LI Juhao^{1*}, GUO Bingli¹, HE Yongqi¹, CHEN Zhangyuan¹, WU Hequan^{1,2}

¹State Key Laboratory of Advanced Optical Communication Systems and Networks, Peking University, Beijing 100871, China

²Chinese Academy of Engineering (CAE), Beijing 100088, China

Abstract: In Elastic Optical Networks (EONs) with flexible bandwidth allocation, the blocking probability is high because of spectral contention. Similar to the functionality of wavelength conversion in Wavelength-Division-Multiplexing (WDM) networks, waveband conversion has been proposed to solve spectral contention in EONs. In this paper, we discuss the design of node architectures for an EON with waveband conversion. Four node architectures with shared Tuneable Waveband Converters (TWBCs) are proposed, and their blocking performances are evaluated by simulation. Simulation results show that the blocking probability of a node is significantly improved by waveband conversion. The sharing efficiency of waveband converters is also investigated. Simulation results show that at the same blocking rate, the node architecture with converters shared per node can save more than 20% waveband converters compared with that of the one with converters shared per link.

Key words: EON; TWBC; node architecture; blocking probability

I. INTRODUCTION

As the rapid growth of online population and the explosion of new applications, the Internet traffic is believed to keep increasing and the bandwidth requirements are more variable. On the other hand, the optical network which supports the Internet traffic is gradually approaching its physical capacity limit [1]. In traditional Wavelength-Division-Multiplexing (WDM)

network, the minimal granularity is a wavelength (100 or 50 GHz), which is not fine enough for efficient bandwidth allocation. With the progress in optical transmission technologies, such as Orthogonal Frequency Division Multiplexing (OFDM) [2] and Single-Carrier Frequency Division Multiplexing (SCFDM) [3], the elastic optical network [4-5] has been proposed to support flexible bandwidth allocation at much finer granularity (10 GHz or less). Furthermore, the spectrum efficiency in Elastic Optical Networks (EONs) is high with small guard bands as subbands are all orthogonal.

However, flexible-bandwidth EONs will cause severe spectral fragmentation and high spectral contention [6]. Waveband conversion has been proposed to solve this problem. The technique principle of waveband conversion [7-9] is similar to that of wavelength conversion in WDM network, which is based on Four-Wave Mixing (FWM). Compared with wavelength conversion in WDM network, the technique requirements of waveband conversion for EONs are more challenging, such as supporting flexible bandwidth and being tuneable at fine granularity. One of the feasible candidates is the Highly Nonlinear Fibre (HNLFF) [10-12]. The feasibility of waveband conversion for spectral defragmentation in EONs has been experimentally demonstrated [13].

In this paper, we focus on the design of node architectures for EON with waveband conversion. Node architectures for WDM networks with wavelength conversion have been exten-

Received: 2013-01-15
Revised: 2013-03-22
Editor: Peter J. Winzer

The node architectures for EONs with waveband conversion are proposed and their blocking performances are compared. TWBCs are used to realise the function of waveband conversion. Simulation results show that the node architecture with TWBC shared by the whole node can achieve the best blocking performance with the fewest converters.

sively studied [14-21]. The node architectures for EONs are different from those for WDM networks because the key devices and switching fabric have been changed. In EONs, waveband converters should support bandwidths varying from one subband (at the granularity of 10 GHz or even less) to one superchannel consisting of tens or even hundreds of subbands. Therefore, it is necessary to discuss the node architectures for EON integrating waveband conversion. We propose and compare four different node architectures, which are distinguished by the placement and sharing schemes of TWBCs. The key components of the four node architectures are analysed. Furthermore, the blocking performances of them are compared by simulation.

The rest of the paper is organised as follows. In Section II, we compare the switching fabric of WDM networks and EONs, and explain why the node architectures with wavelength conversion proposed in WDM networks are not applicable in EONs. In Section III, four node architectures for EONs with waveband conversion are proposed and compared in detail. The blocking performances of the four node architectures are evaluated by simulation in Section IV. Finally, the last section is the conclusion.

II. SWITCHING FABRIC OF WDM NETWORKS AND EONS

In this section, we briefly compare the switching fabric of WDM networks and EONs. In WDM networks, the wavelengths are fixed with the standard ITU-T frequency grids. The switching fabric is usually composed of Multiplexer (MUX), Demultiplexer (DEMUX) and Photonic Cross-Connection (PXC) with large port counts [21]. As shown in Figure 1 (a), the key device of the switching fabric is $(N*W) \times (N*W)$ PXC, where N is the node degree and W is the number of wavelengths in one input/output link. Since the cost of PXC is related with the port count, multi-granular optical switching has been proposed to reduce the port count [22].

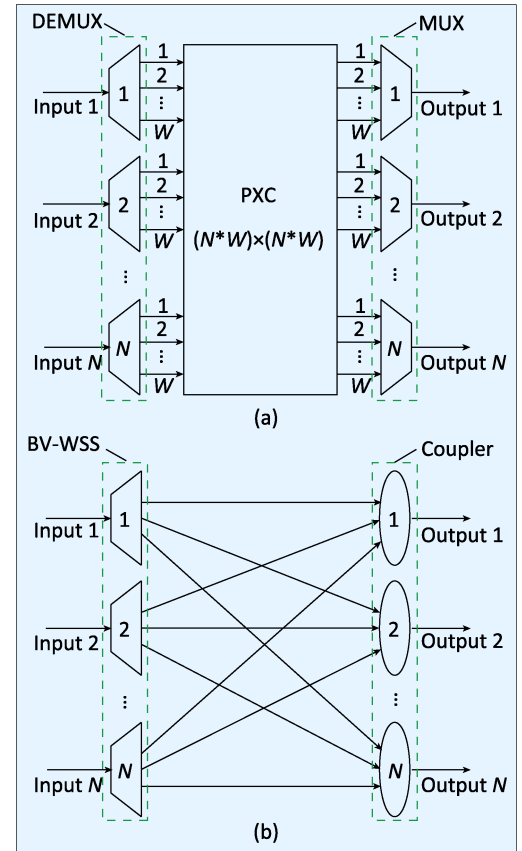


Fig.1 Comparison of switching fabrics (a) WDM networks (b) EONs

In WDM networks, the wavelength converters can be integrated with the switching fabric easily. Two node architectures for WDM networks with wavelength conversion are shown in Figure 2 (a) and 2 (b), where Wavelength Converters (WCs) are dedicated and shared by the node [20]. In the dedicated approach (shown in Figure 2 (a)), each wavelength of the input links has one dedicated WC. For a node with N input links and W wavelengths for each link, the total number of WCs required is $N*W$. In the shared approach (shown in Figure 2 (b)), a limited number of WCs are shared by all the input links in the node. With $N*M$ shared WCs, the port count of PXC should increase from $N*W$ to $N*(W+M)$. Generally, a relatively smaller number of WCs in the shared approach can approximate the blocking performance with the dedicated approach, which means the WCs are more efficiently used in the shared approach. The cost is that the PXC should support a larger port count, which is

a trade-off.

In EONs, wavebands are bandwidth-flexible with mini-grid or even gridless [23]. Therefore, the conventional switching fabric composed of DEMUX, MUX and PXC in WDM networks is not applicable in EONs. Bandwidth-Variable Waveband Selective Switch (BV-WSS) [4] is introduced to switch wavebands with flexible bandwidth. As shown in Figure 1 (b), the switching fabric in EONs is composed of BV-WSSs and couplers. There is one BV-WSS in each input link, where wavebands with different output links are separated. At the output links, the wavebands from different inputs are combined by a coupler. In this switching fabric, in each input link, only the wavebands for different output links are separated, which is unlike the case in WDM networks. The wavebands with same output link are switched as a whole unit. However, if waveband conversion is introduced, these wavebands should be separated before they can be converted. Therefore, additional devices should be introduced to integrate the TWBCs with the switching fabric in EONs.

III. NODE ARCHITECTURES FOR EONS WITH WAVEBAND CONVERSION

In this section, we investigate the design of node architectures for EONs with waveband conversion, including node architectures, structural contentions and key devices.

The basic parameters of the node are set as follows. The node degree is N , which means there are N input links and N output links. The node is equipped with $M*N$ TWBCs, i.e., M TWBCs for each input link. For simplicity, the node is merely a switching node, while the add/drop function is not considered.

3.1 Node architectures

In EONs, TWBCs should be shared in the node because of the high cost. Similar to the sharing schemes of wavelength converters in WDM networks [17], there are two approaches to share the TWBCs: shared per link and shared per node. In the former, TWBCs are shared only by each input/output link, while

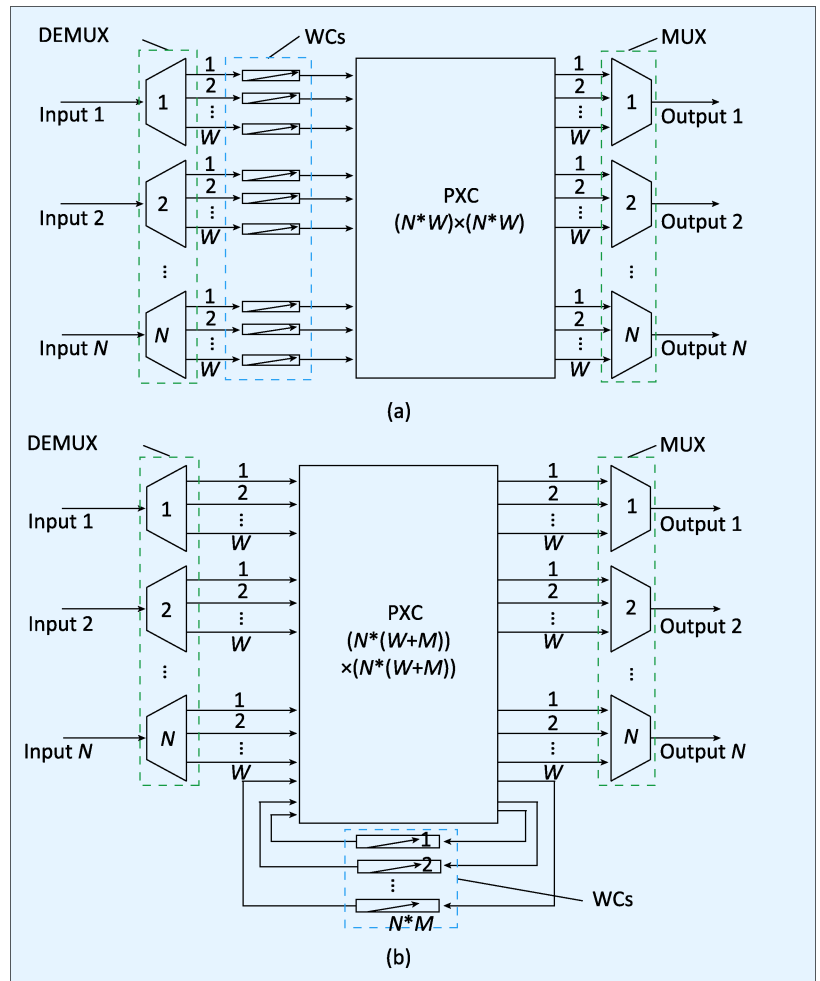


Fig.2 Node architectures of WDM network with wavelength conversion (a) dedicated (b) shared

in the latter TWBCs are shared by the whole node. Based on the placement and sharing schemes of TWBCs, we propose four node architectures depicted in Figure 3 (a-d), which are denoted as Node Architecture I (NA-I) to NA-IV. Among the four node architectures, the first three are classified as “shared per link”, and the last one is “shared per node”.

NA-I has been proposed in Ref. [13], which focuses on spectral defragmentation. As shown in Figure 3 (a), in this architecture, waveband conversion is performed before switching, while the basic switching fabric remains unchanged. At each input link, the wavebands which need to be converted are firstly separated from the unconverted wavebands and sent to the TWBC pool for conversion. After conversion, the converted wavebands are converged back with the unconverted wavebands

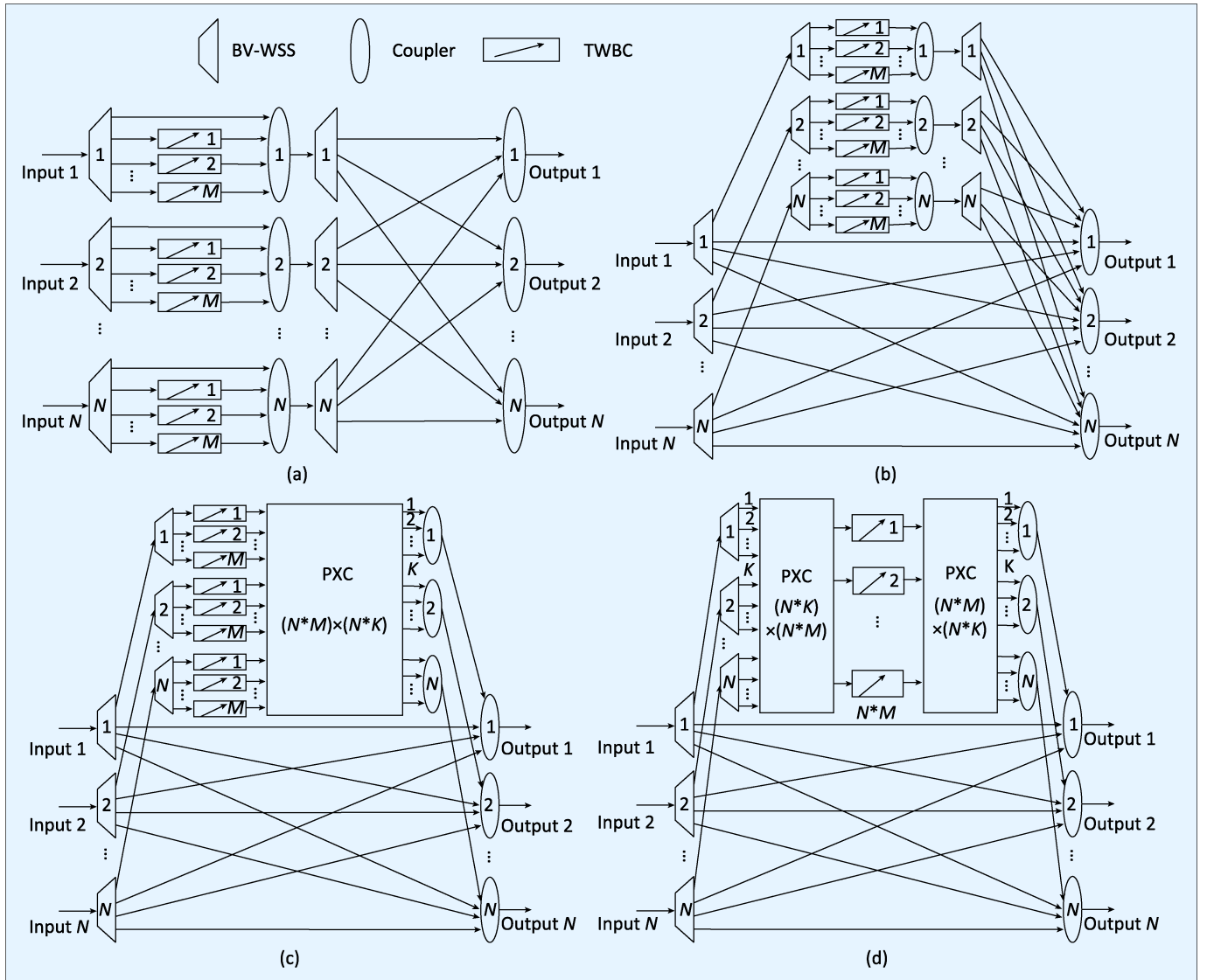


Fig.3 Node architectures for EONs with waveband conversion (a) NA-I (b) NA-II (c) NA-III (d) NA-IV

from the same input link by a coupler. Finally the defragmented signals are switched by the switching fabric which consists of BV-WSSs and couplers.

NA-II is a modification of NA-I, where waveband conversion is integrated with the switching fabric. As shown in Figure 3 (b), the unconverted wavebands are directly switched to the output links, while the wavebands which need to be converted are switched to the TWBC pool. After conversion, the converted wavebands of the same input link are firstly converged by a coupler and then switched to the output links by a BV-WSS according to their destinations.

NA-III is almost the same with NA-II, exc-

cept the switching components after conversion. As shown in Figure 3 (c), the N sets of couplers and BV-WSSs in NA-II are replaced by an $(N*M) \times (N*K)$ PXC in NA-III. The parameter K represents the maximum number of converted wavebands allowed for each output link.

NA-IV is different from the above three node architectures, in which TWBCs are shared by all the input links in the node. As shown in Figure 3 (d), compared with NA-III, an additional $(N*K) \times (N*M)$ PXC is placed before the TWBC pool to switch the wavebands which need to be converted to the corresponding converters. Besides the representation described in NA-III, the parameter K in NA-IV

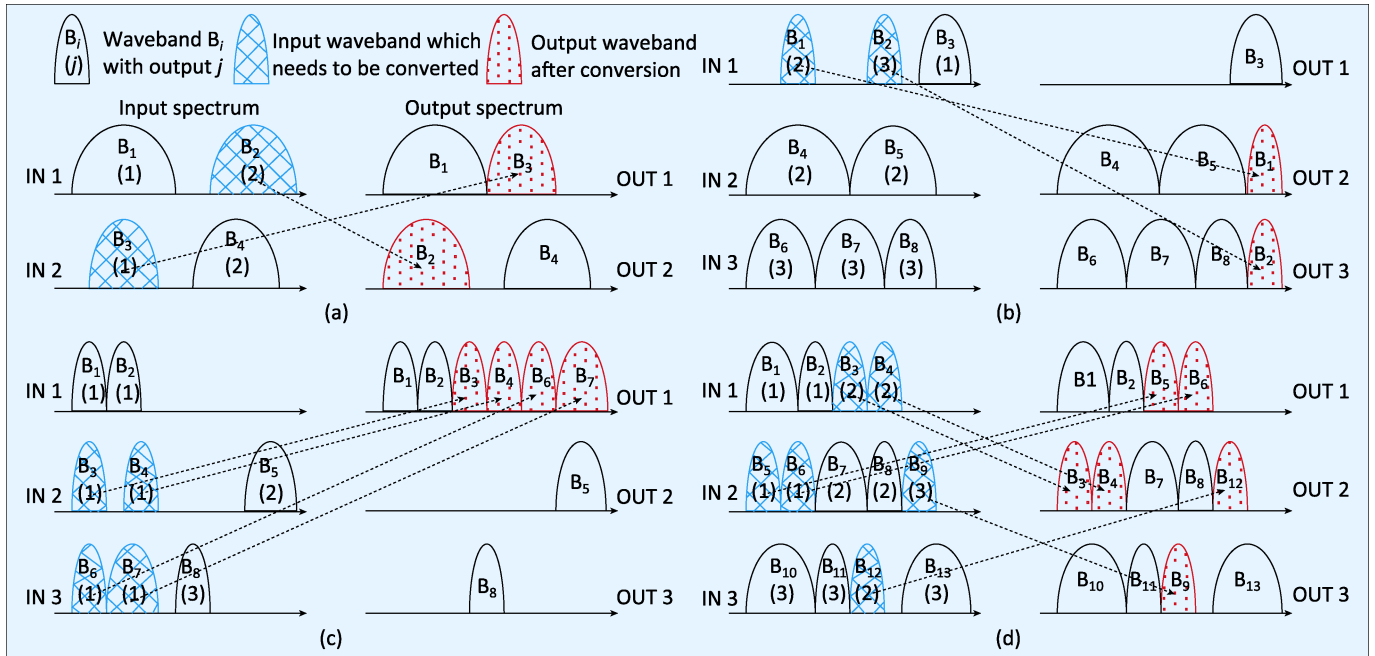


Fig.4 Structural contention in the proposed node architectures (a) SC-1 (b) SC-2 (c) SC-3 (d) SC-4

also represents the maximum number of wavebands allowed to be converted for each input link. If K is equal to M , which means no more than M wavebands are allowed to be converted for each input link, this node architecture would be degenerated to the case of shared per link as NA-III. When the value of K increases, the advantage of NA-IV will be enhanced.

3.2 Structural Contention

In this subsection, we analyse the blocking performance of the proposed node architectures. The ideal node architecture with full waveband conversion capability is chosen as the reference. Compared with the ideal node architecture, all the node structures described in Section 3.1 have some types of structural contention. Four types of structural contention are shown in Figure 4 to illustrate the different blocking performances of the four node architectures. In this case, we assume $M=2$ and $K=3$. In the figures, the left side shows the spectrum of input links before switching and waveband conversion, and the right side shows the spectrum of output links after switching and waveband conversion in the ideal node architecture.

The first type of Structural Contention (SC-1)

is the contention between unconverted wavebands and converted wavebands in the same input link, which is shown in Figure 4 (a). There are two input links and two output links in this example. Since the wavebands B_1 and B_3 have the same Output Link (OUT 1) with overlapping spectrums, one of them (e.g., B_3) should be converted to the unused spectrum. The scenario for waveband B_2 and B_4 is similar. The four wavebands can be switched without contention in the ideal case as shown in Figure 4 (a). However, it cannot be realised in NA-I since the converted wavebands need to be multiplexed back with the unconverted ones before switching. SC-1 only exists in NA-I and can be avoided in other three node architectures, since converted wavebands and unconverted wavebands are separately switched in the latter three ones.

The second type of Structural Contention (SC-2) is the contention between the converted wavebands in the same link, which is shown in Figure 4 (b). There are three input links and three output links in this example. The wavebands B_1 and B_2 from input 1 are to be switched to outputs 2 and 3 accordingly. As shown in Figure 4 (b), there are unused spectrums in outputs 2 and 3 which are large

Table I Structural Contention in four node architectures

	SC-1*	SC-2	SC-3	SC-4
NA-I	√	√	×	√
NA-II	×	√	×	√
NA-III	×	×	√	√
NA-IV	×	×	√	×

*The notions SC-1, SC-2, SC-3 and SC-4 in the header row denote the four types of Structural Contention described in Figure 4 accordingly.

Table II Key devices in four node architectures

	TWBC	BV-WSS	PXC
NA-I	$M*N$	$N: 1 \times N^*$; $N: 1 \times (M+1)$	0
NA-II	$M*N$	$N: 1 \times N$; $N: 1 \times M$; $N: 1 \times (N+1)$	0
NA-III	$M*N$	$N: 1 \times M$; $N: 1 \times (N+1)$	1: $(N*M) \times (N*K)$
NA-IV	$M*N$	$N: 1 \times K$; $N: 1 \times (N+1)$	2: $(N*M) \times (N*K)$

The notion " $N: 1 \times N^$ " in the table represents N BV-WSS with port $1 \times N$.

enough for the two wavebands. However, since the wavebands B_1 and B_2 after conversion have overlapping spectrums, the waveband conversion cannot be realised in NA-I and NA-II as converted wavebands from the same link are firstly converged by a coupler before switching. SC-2 exists in NA-I and NA-II, and can be avoided in NA-III and NA-IV by introducing the output PXC.

The third type of Structural Contention (SC-3) is the contention because of the port count limitation of the output PXC, which is shown in Figure 4 (c). In this example, there are six wavebands (B_1, B_2, B_3, B_4, B_6 and B_7) which are to be switched to output 1. The three wavebands B_1, B_3 and B_6 have common spectrums, thus two of them need to be converted. The situation for wavebands B_2, B_4 and B_7 is the same. Therefore, at least four converted wavebands should be switched to output link 1. However, the maximum number of converted wavebands for each output link in NA-III and NA-IV cannot exceed three as $K=3$ is assumed. Therefore, in this example, there is contention in NA-III and NA-IV although the number of wavebands which need to be converted in each input link does not exceed the number of TWBCs. SC-3 exists in NA-III and NA-IV, and can be eliminated if we increase the value of K .

The fourth type of Structural Contention (SC-4) is the contention because of the limita-

tion of TWBCs in each input link, which is shown in Figure 4 (d). In this example, there are six wavebands which need to be converted, among which two (B_3 and B_4) are from input 1, three (B_5, B_6 and B_9) from input 2 and one (B_{12}) from input 3. In NA-I, NA-II and NA-III, TWBCs are shared by each input link and a maximum of two wavebands are allowed to be converted in each input link as $M=2$ is assumed. Therefore, one of the three wavebands in input 2 should be blocked in these three node architectures. SC-4 exists in NA-I, NA-II and NA-III, and can be avoided in NA-IV since TWBCs are shared by all input links in the node with the input PXC.

As a summary, the structural contention in the four proposed node architectures is shown in Table I. From the table, we can find that the blocking performance of NA-I is the worst which suffers from three types of Structural Contention (SC-1, SC-2 and SC-4). The blocking performance of NA-IV is the best with only one type (SC-3). The blocking performances of NA-II and NA-III are close with two types of structural contention. SC-2 and SC-4 exist in NA-II, while SC-3 and SC-4 exist in NA-III.

3.3 Key devices

The components used in the proposed four node architectures are compared in this subsection. For simplicity, only three key devices are listed in Table II: TWBC, BV-WSS, and PXC. The number of TWBCs in the four node architectures is the same, which is $N*M$ for one node (or M for each input link). The other two devices: BV-WSS and PXC, are both port-sensitive, i.e., the cost of them are sensitive to port counts. Therefore, both the number and port counts of the components are shown in Table II. Despite the difference in port counts, the number of BV-WSSs required in NA-II is $3*N$, which is the largest of the four, while the other three only need $2*N$. The PXCs are only required in NA-III and NA-IV, the number of which are 1 and 2 accordingly.

The BV-WSSs are used in all the four node architectures, which demultiplex wavebands

with flexible bandwidths. One of the feasible technologies of BV-WSSs is the Liquid Crystal (LC) [24]. In this paper, five types of BV-WSSs with different port counts are required: $1 \times N$, $1 \times (N+1)$, $1 \times M$, $1 \times (M+1)$ and $1 \times K$. Generally, the value N (i.e., node degree) is small ($N=4$ or 5 is enough for most optical networks). The parameter M and K are also not large. As evaluated in the simulation in the next section, $M=12$ and $K=16$ are sufficient in NA-IV to approximate the blocking performance of full waveband conversion. Therefore, the BV-WSS with port 1×16 is sufficient to support the node architectures proposed in this paper. The scalability of BV-WSSs can be realised by parallel BV-WSSs with smaller port counts. For example, a BV-WSS with port 1×16 can be realised by one 1×4 splitter and four BV-WSSs with port 1×4 .

The PXC with port $(N \times M) \times (N \times K)$ are used in NA-III and NA-IV to share the limited number of TWBCs more effectively by all the input/output links in the node. From the view of input links, with $K > M$, some input links can support more than M but no more than K wavebands to be converted, providing that the total number of wavebands which need to be converted is no more than $N \times M$. The asymmetric PXC can save port counts in one side compared with symmetric PXC. Nevertheless, they are not indispensable and can be replaced with symmetric ones. For example, the asymmetric PXC with port $(N \times M) \times (N \times K)$ (with $K > M$) used in NA-III and NA-IV can be realised by symmetric ones with port $(N \times K) \times (N \times K)$. There are many switching technologies [25] to realise the PXC, such as MEMS [26]. In our example, with node degree $N=4$, $M=12$ and $K=16$, the PXC with port 64×48 (or the symmetric one with port 64×64) is sufficient. For scalability, the port counts of PXC can be set one time larger (i.e., 128×96 for asymmetric PXC or 128×128 for symmetric one).

IV. PERFORMANCE EVALUATION

The performances of blocking probability in the proposed four node architectures are compared by simulation in this section. We assume

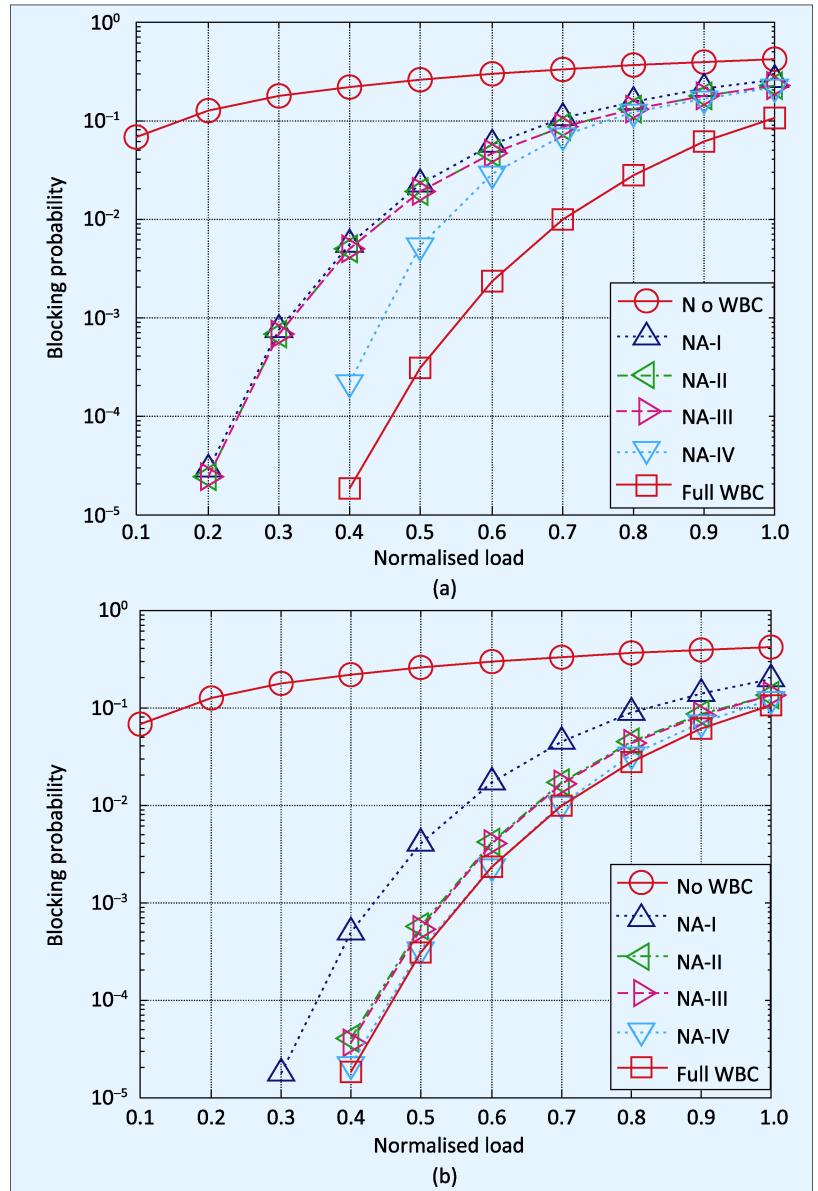


Fig.5 Blocking probability vs. normalised traffic load in two scenarios (a) $M=5$, $K=10$ (b) $M=10$, $K=20$

that the link consists of 400 subbands with granularity of 10 GHz. The traffic load arrives according to Poisson arrival, with bandwidth varying from 1 to 19 subbands, on the average of 10 subbands. The traffic is uniformly distributed, i.e., the traffic from one input link has the same probability to be switched to the N output links. The node degree N is set to 4 in the simulation.

The blocking probabilities of the four node architectures with different traffic loads are shown in Figure 5. The blocking probabilities of the two special cases — no Waveband

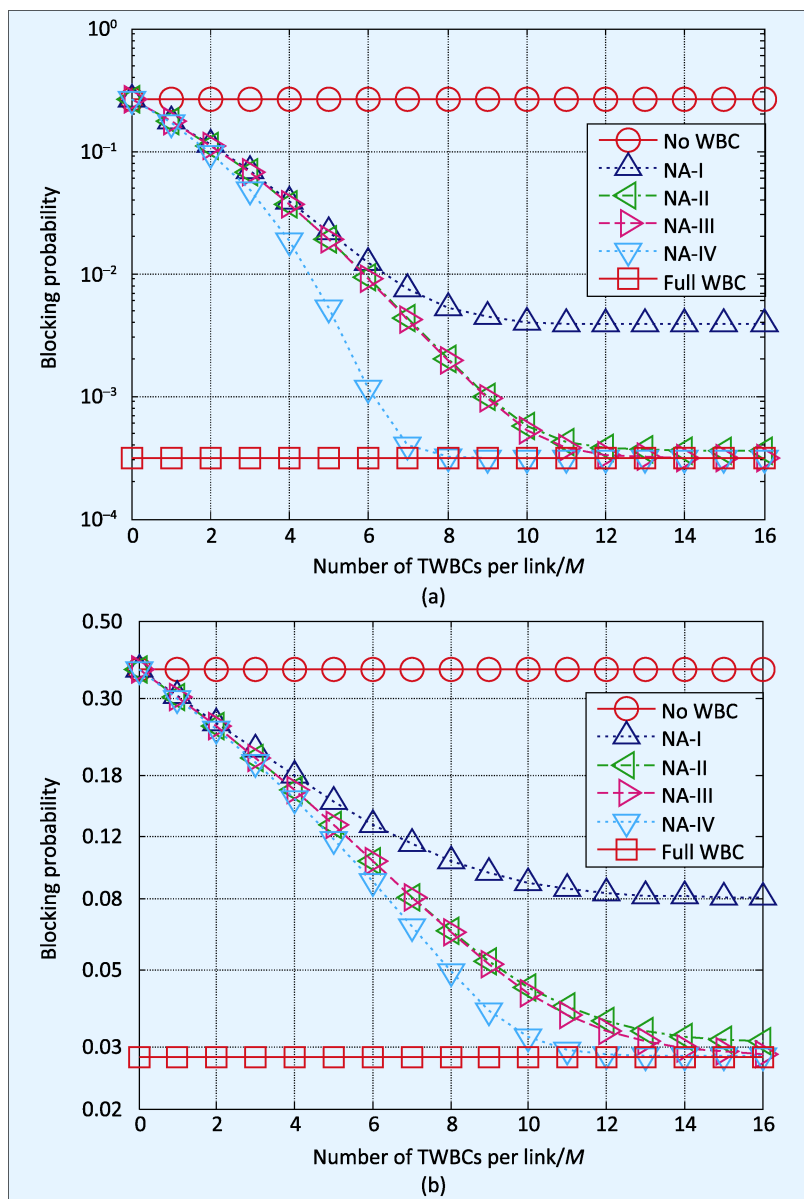


Fig.6 Blocking probability vs. number of TWBCs for median and heavy load (a) $\rho=0.5$ (b) $\rho=0.8$

Conversion (no WBC) and full WBC are also shown as a reference. The results in Figure 5 (a) and 5 (b) are obtained with parameters $M=5$, $K=10$ and $M=10$, $K=20$ respectively. From Figure 5 (a), we can see that the blocking performance of NA-IV is the best of the four, while the other three are almost the same. In Figure 5 (b), the performance of NA-IV is also the best and that of NA-I is the worst, while the other two are still close. This is reasonable according to the blocking analysis in the previous section. Compared with the case of no WBC, the blocking probabilities of the

four proposed node architectures with WBC are all improved significantly. For example, at traffic load $\rho=0.5$, the block probability is reduced 1-2 magnitudes in Figure 5 (a) and 2-3 magnitudes in Figure 5 (b).

Figure 6 shows the blocking probability versus the number of TWBCs for each link (denoted as M). The results shown in Figure 6 (a) and 6 (b) are simulated at median ($\rho=0.5$) and heavy ($\rho=0.8$) traffic loads respectively. For all the four node architectures, the blocking probabilities decrease when the number of TWBCs increases. When M is zero (i.e., no WBC is implemented), the blocking probabilities of the four are the same, which is equal to that of no WBC. When M increases, the blocking probabilities of the four node architectures decrease dramatically at the beginning and become stable gradually. As depicted in the previous section, NA-I and NA-II have inevitable structural contention, which cannot be eliminated by the increment of M . Therefore, the blocking probabilities of NA-I and NA-II cannot achieve that of full WBC however the value of M is increased. The floor level of NA-II is much lower than that of NA-I, which indicates the probability of structural contention in NA-I is much higher. On the other hand, the blocking probability of NA-III and NA-IV can achieve that of full WBC if M is large enough.

To evaluate the sharing efficiency of TWBCs, the sufficient number of TWBCs required for each input link is defined as the minimal value of M at which the blocking probability reaches that of full WBC (with relative difference less than 5%). The sufficient number of TWBCs for NA-III and NA-IV is shown in Figure 7. As we can see, the sufficient number is related to the traffic load, which is large when the traffic load is heavy. It is because that for heavy traffic, the contention occurs more frequently and thus more TWBCs are needed. The sufficient number is also related to the node architectures. In Figure 7, we can see that at the heavy load ($\rho=1$), the sufficient number of TWBCs is 12 in NA-IV, but is 15 in NA-III, which means a number of 20% TWBCs are

saved in NA-IV compared with that in NA-III. The reason is that the TWBCs in NA-IV are more effectively used by sharing in the whole node.

The blocking probability versus the port number per link in PXC (i.e., the parameter K) is shown in Figure 8. Among the four node architectures, the blocking performances of NA-III and NA-IV are related to K . For clarification, only the performances of NA-II, NA-III, NA-IV and full WBC are shown in Figure 8. In the simulation, the value of M is fixed at 10, and the value of K varies from 10 to 20. When K is equal to M , the performances of NA-III and NA-IV are the same, as the number of TWBCs for each link in NA-IV is also no more than M , which is the same in NA-III. Therefore, the blocking probabilities of NA-III and NA-IV are the same when $K=10$ as shown in Figure 8. We can also find that the blocking probability of NA-II is lower than that of NA-III and NA-IV when K is small. It is because that the output port number of NA-III and NA-IV is limited by K , which would introduce high probability of SC-3 described in the previous section. The blocking probabilities of NA-III and NA-IV decrease when K increases. The blocking probability does not decrease any more if K is large enough. The sufficient number of K is around 16 in both median ($\rho=0.5$) and heavy ($\rho=0.8$) traffic loads. As shown in Figure 8 (a), the blocking probability of NA-IV can reach the case of full WBC at median traffic load ($\rho=0.5$). However, at heavy load ($\rho=0.8$) as shown in Figure 8 (b), the blocking probability of NA-IV is always higher than that of full WBC however K is increased. This is because of the limitation on M , which has been discussed in the previous paragraph.

V. CONCLUSION

The node architectures for EONs with waveband conversion were discussed in this paper. Based on the placement and sharing schemes of TWBCs, four node architectures were proposed and their performances are compared by simulation.

From the simulation, we found that WBC

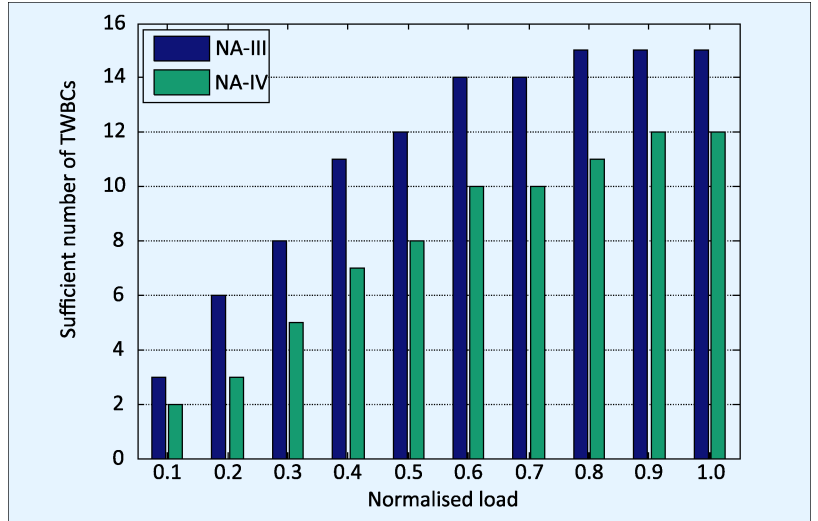


Fig.7 Sufficient number of TWBCs for NA-III and NA-IV

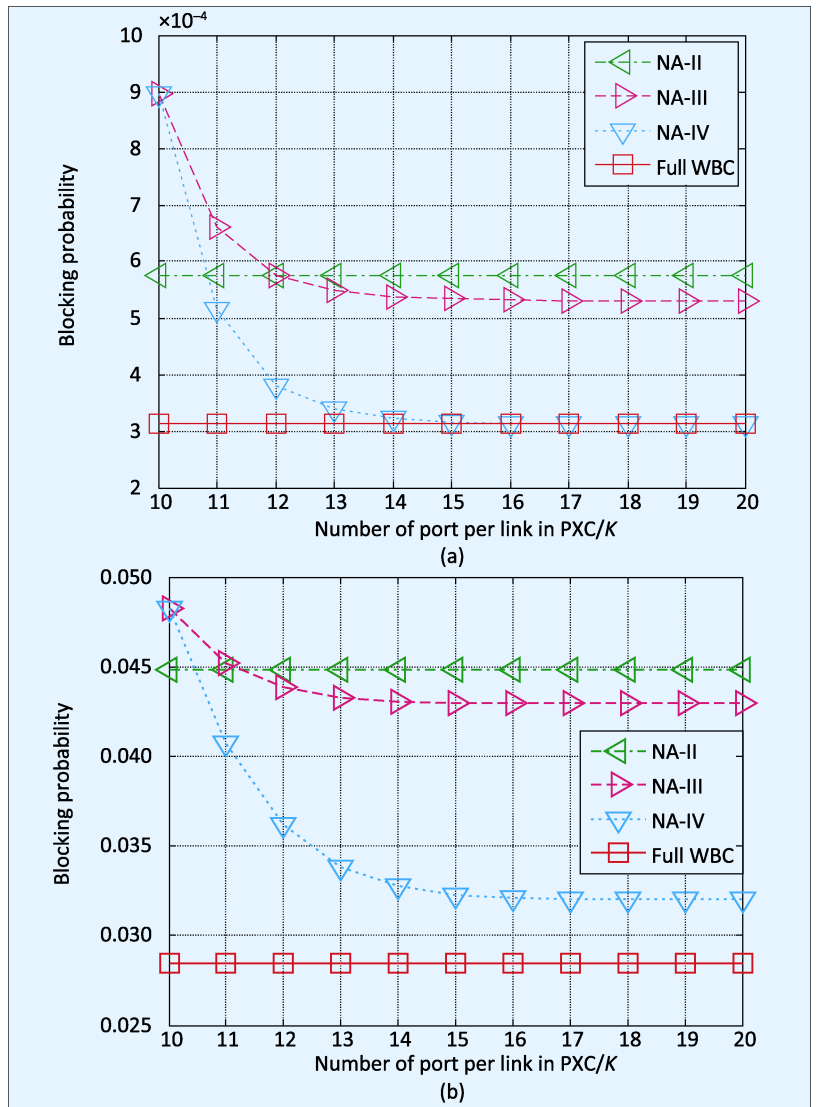


Fig.8 Blocking probability vs. port number in PXC for median and heavy load (a) $\rho=0.5$ (b) $\rho=0.8$

can improve the blocking probabilities of the node significantly, with reduction of 2-4 magnitudes at light load ($\rho < 0.5$). Among the four node architectures, the blocking performance of NA-IV is the best, and that of NA-I is the worst. The node architectures of NA-I and NA-II have inevitable structural contention, and cannot achieve the best blocking probability as that of full WBC. On the contrary, the node architectures of NA-III and NA-IV can achieve the blocking probability as that of full WBC in case that the number of TWBCs (M) and port number in PXC (K) are large enough. In our simulation settings, to achieve the blocking probability of full WBC (with relative difference less than 5%), $M=12$ and $K=16$ are required in NA-IV, while $M=15$ and $K=16$ are required in NA-III, which indicates that the TWBCs are more effectively used in NA-IV (shared per node) than in NA-III (shared per link).

ACKNOWLEDGEMENT

This work was supported by the National Key Basic Research Program of China (973 Program) under Grants No. 2010CB328201, No. 2010CB328202; the National Natural Science Foundation of China under Grants No. 60907030, No. 61275071, No. 60736003, No. 60931160439; and the National High Technical Research and Development Program of China (863 Program) under Grant No. 2011AA01A106.

References

[1] ESSIAMBRE R J, KRAMER G, WINZER P J, *et al.* Capacity Limits of Optical Fibre Networks[J]. *Journal of Lightwave Technology*, 2010, 28(4): 662-701.

[2] ARMSTRONG J. OFDM for Optical Communications[J]. *Journal of Lightwave Technology*, 2009, 27(3): 189-204.

[3] ZHAO Chunxu, CHEN Yuanxiang, ZHANG Su, *et al.* Experimental Demonstration of 1.08 Tb/s PDM CO-SCFDM Transmission over 3170 km SSMF[J]. *Optics Express*, 2012, 20(2): 787-793.

[4] JINNO M, TAKARA H, KOZICKI B, *et al.* Spectrum-Efficient and Scalable Elastic Optical Path Network: Architecture, Benefits, and Enabling Technologies[J]. *IEEE Communications Magazine*, 2009, 47(11): 66-73.

[5] GERSTEL O, JINNO M, LORD A, *et al.* Elastic Optical Networking: A New Dawn for the Optical Layer?[J]. *IEEE Communications Magazine*, 2012, 50(2): s12-s20.

[6] THIAGARAJAN S, FRANKEL M, BOERTJES D. Spectrum Efficient Super-Channels in Dynamic Flexible Grid Networks — A Blocking Analysis[C]// *Proceedings of 2011 Optical Fibre Communication Conference and Exposition, and the National Fibre Optic Engineers Conference (OFC/NFOEC): March 6-10, 2011. Los Angeles, CA, USA, 2011: 1-3.*

[7] POLITI C, KLONIDIS D, O'MAHONY M J. Waveband Converters Based on Four-Wave Mixing in SOAs[J]. *Journal of Lightwave Technology*, 2006, 24(3): 1203-1217.

[8] SONG Hongbin, TADANAGA O, UMEKI T, *et al.* Phase-Transparent Flexible Waveband Conversion of 43 Gb/s RZ-DQPSK Signals Using Multiple-QPM-LN Waveguides[J]. *Optics Express*, 2010, 18(15): 15332-15337.

[9] TOMITA I, UMEKI T, TADANAGA O, *et al.* Apodized Multiple Quasi-Phase-Matched LiNbO₃ Device for Low-Cross-Talk Waveband Conversion[J]. *Optics Letters*, 2010, 35(6): 805-807.

[10] TAKAHASHI M, HIROISHI J, TADAKUMA M, *et al.* FWM Wavelength Conversion with over 60 nm of 0 dB Conversion Bandwidth by SBS-Suppressed HNLFC[J]// *Proceedings of Conference on Optical Fibre Communication (OFC 2009): March 22-26, 2009. San Diego, CA, USA, 2009: 1-3.*

[11] OSHIBA S, MORITOMO R. All-Optical Arbitrary Wavelength Conversion with Signal Regeneration Based on Slicing of Supercontinuum Spectrum[C]// *Proceedings of 2009 IEEE/LEOS Winter Topicals Meeting Series: January 12-14, 2009. Innsbruck, Austria, 2009: 256-257.*

[12] XU Xing, ZHANG Chi, YUK T I, *et al.* Stabilised Wide-Band Wavelength Conversion Enabled by CW-Triggered Supercontinuum[J]. *IEEE Photonics Technology Letters*, 2012, 24(20): 1886-1889.

[13] GEISLER D J, YIN Yawei, WEN Ke, *et al.* Demonstration of Spectral Defragmentation in Flexible Bandwidth Optical Networking by FWM [J]. *IEEE Photonics Technology Letters*, 2011, 23(24): 1893-1895.

[14] LI Deying, JIA Xiaohua. Allocating Wavelength Converters in Shared-Per-Link Structure in WDM Networks[J]. *IET Communications*, 2002, 149(3): 185-188.

[15] ERAMO V, LISTANTI M, PACIFICI P. A Comparison Study on the Number of Wavelength Converters Needed in Synchronous and Asynchronous All-Optical Switching Architectures [J]. *Journal of Lightwave Technology*, 2003, 21(2): 340-355.

- [16] ZHANG Zhenghao, YANG Yuanyuan. On-Line Optimal Wavelength Assignment in WDM Networks With Shared Wavelength Converter Pool[J]. *IEEE/ACM Transactions on Networking*, 2007, 15(1): 234-245.
- [17] YAN Fangfang, HU Weisheng, SUN Weiqiang, *et al.* Efficient Sharing of Fixed Wavelength Converters in Clos-Type Wavelength Interchanging Cross Connects[J]. *Journal of Lightwave Technology*, 2009, 27(19): 4189-4197.
- [18] YOO S B. Wavelength Conversion Technologies for WDM Network Applications[J]. *Journal of Lightwave Technology*, 1996, 14(6): 955-966.
- [19] RAMAMURTHY B, MUKHERJEE B. Wavelength Conversion in WDM Networking[J]. *IEEE Journal on Selected Areas in Communications*, 1998, 16(7): 1061-1073.
- [20] PAPADIMITRIOU G I, PAPAZOGLU C, POMPORTSIS A S. Optical Switching: Switch Fabrics, Techniques, and Architectures[J]. *Journal of Lightwave Technology*, 2003, 21(2): 384-405.
- [21] WILFONG G, MIKKELSEN B, DOERR C, *et al.* WDM Cross-Connect Architectures with Reduced Complexity[J]. *Journal of Lightwave Technology*, 1999, 17(10): 1732-1741.
- [22] WANG Yang, CAO Xiaojun. Multi-Granular Optical Switching: A Classified Overview for the Past and Future[J]. *IEEE Communications Surveys & Tutorials*, 2012, 14(3): 698-713.
- [23] SHEN Gangxiang, YANG Qi. From Coarse Grid to Mini-Grid to Gridless: How much Can Gridless Help Contentionless?[C]// *Proceedings of 2011 Optical Fibre Communication Conference and Exposition, and the National Fibre Optic Engineers Conference (OFC/NFOEC): March 6-10, 2011. Los Angeles, CA, USA, 2011: 1-3.*
- [24] BAXTER G, FRISKEN S, ABAKOUMOV D, *et al.* Highly Programmable Wavelength Selective Switch Based on Liquid Crystal on Silicon Switching Elements[C]// *Proceedings of 2006 Optical Fibre Communication Conference and Exposition, and the National Fibre Optic Engineers Conference (OFC/NFOEC): March 5-20, 2006. Anaheim, CA, USA, 2006.*
- [25] MA Xiaohua, KUO Gengsheng. Optical Switching Technology Comparison: Optical MEMS vs. Other Technologies[J]. *IEEE Communications Magazine*, 2003, 41(11): S16-S23.
- [26] YANO M, YAMAGISHI F, TSUDA T. Optical MEMS for Photonic Switching-Compact and Stable Optical Crossconnect Switches for Simple, Fast, and Flexible Wavelength Applications in Recent Photonic Networks[J]. *IEEE Journal of Selected Topics in Quantum Electronics*, 2005, 11(2): 383-394.

Biographies

ZHANG Ping, is currently pursuing the Ph.D. degree at the State Key Laboratory of Advanced Optical Communication Systems and Networks, Peking University, Beijing, China. He received his B.S. degree in electronics from Peking University, China in 2005. His current research is in high speed optical network and switching. Email: zhangping1224@gmail.com

Li Juhao, Associate Professor at the State Key Laboratory of Advanced Optical Communication Systems and Networks, Peking University, Beijing, China. He received the B.S. and Ph.D. degrees from Peking University, China in 1999 and 2009, respectively. From 1999 to 2000, he engaged in ZTE Corporation. His current research interests include optical switching network, passive optical network and high-speed optical fibre transmission system. *The corresponding author. Email: juhao_li@pku.edu.cn

GUO Bingli, postdoctoral researcher at the State Key Laboratory of Advanced Optical Communication Systems and Networks, Peking University, Beijing, China. He received his B.E. degree in communication engineering from Jilin University, Changchun, China in 2005, and Ph.D. degree in Beijing University of Posts and Telecommunications, Beijing, China in 2011. His current research interests include control and management technologies in future optical networks.

HE Yongqi, Professor at the State Key Laboratory of Advanced Optical Communication Systems and Networks, Peking University, Beijing, China. He received his B.S. degree in physics from Beijing Normal University, China in 1983, M.S. degree in optical communications from Beijing University of Posts and Telecommunications, China in 1987, and Ph.D. degree in optical communications from Technical University of Denmark, Denmark in 1996. His research interests include optical transport networks, high speed DWDM systems and optical processing.

CHEN Zhangyuan, Professor at the State Key Laboratory of Advanced Optical Communication Systems and Networks, Peking University, Beijing, China. He received his B.S., M.S. and Ph.D. degrees from Peking University, China in 1991, 1994 and 1997 respectively. His main research interest is in the area of optical communications and photonic devices.

WU Hequan, Professor at the State Key Laboratory of Advanced Optical Communication Systems and Networks in Peking University, and Academician of Chinese Academy of Engineering (CAE), China. He graduated from Wuhan Posts and Telecommunications Institute, China in 1964.